Interfacial Crack Arrest in Sandwich Beams Subjected to Fatigue Loading using a Novel Crack Arresting Device – Numerical modelling

Martakos, Georgios; Andreasen, Jens Henrik; Berggreen, C.; Thomsen, Ole Thybo

Published in:
Journal of Sandwich Structures & Materials

DOI (link to publication from Publisher):
10.1177/1099636217695058

Publication date:
2019

Document Version
Accepted author manuscript, peer reviewed version

Corresponding Author:

Ole T. Thomsen, Faculty of Engineering and the Environment, University of Southampton, Highfield, Southampton, UK

Email: o.thomsen@soton.ac.uk , web page: http://www.soton.ac.uk/engineering/

Interfacial Crack Arrest in Sandwich Beams Subjected to Fatigue Loading using a Novel Crack Arresting Device – Numerical modelling

G. Martakos[1], J.H. Andreasen[1], C. Berggreen[2], O.T. Thomsen[3,1]

[1]Department of Mechanical and Manufacturing Engineering, Aalborg University

Fibigerstræde 16, DK-9220 Aalborg East, Denmark

Email: {gm,jha, ott}@aau.dk, web page: http://www.aau.dk

[3]Department of Mechanical Engineering, Technical University of Denmark

Nils Koppels Allé, Building 403, DK-2800 Kgs. Lyngby, Denmark

Email: cbe@mek.dtu.dk, web page: http://www.mek.dtu.dk

[3]Faculty of Engineering and the Environment,
University of Southampton, Highfield, Southampton, UK

Email: o.thomsen@soton.ac.uk , web page: http://www.soton.ac.uk/engineering/

Abstract

A novel crack arresting device is implemented in foam cored composite sandwich beams and tested using the Sandwich Tear Test (STT) configuration. A Finite Element Model of the setup is developed, and the predictions are correlated with observations and results from a recently conducted experimental fatigue test study. Based on a linear elastic fracture mechanics approach, the developed FE model is utilized to simulate crack propagation and arrest in foam cored sandwich beam specimens subjected to fatigue loading conditions. The effect of the crack arresters on the fatigue life is analysed, and the predictive results are subsequently compared with the observations from the

previously conducted fatigue tests. The FE model predicts the energy release rate and the mode mixity based on the derived crack surface displacements, utilizing algorithms for the prediction of accelerated fatigue crack growth as well as the strain field evolution in the vicinity of the crack tip on the surface of the sandwich specimens. It is further shown that the developed finite element analysis methodology can be used to gain a deeper insight onto the physics and behavioral characteristics of the novel peel stopper concept, as well as a design tool that can be used for the implementation of crack arresting devises in engineering applications of sandwich components and structures.

Keywords

Sandwich structures, Finite Element Analysis, Composites, Fracture Mechanics, Fatigue

INTRODUCTION

Sandwich structures represent a special form of laminated composites comprising stiff and thin face-sheets separated by and bonded to either side of a light and compliant core material. The resulting layered sandwich element or structure displays very high stiffness and strength to weight ratios [1]. Structurally, the face-sheets are responsible for carrying the in-plane stresses and the bending loads, while the core carries the out of plane shear stresses. Sandwich structures are notoriously sensitive to debonding or interfacial cracking of the adhesive bond layers that connect the face-sheets to the core material. When such interface cracks or debonds propagate this may lead to a significant loss (complete loss as a worst case scenario) of structural integrity, leading to premature structural failure or collapse. Such debonds may be caused by in-service loads such as local/concentrated external loads and impact loads, but may also be induced as defects during the manufacturing process (such as e.g. dry spots and resin voids). Ideally face-sheet/core debonds should not occur at all, but since this is impossible to achieve for real industrial scale sandwich structures which may also include safety critical applications, there is a need to develop and introduce design methodologies able to take account of the existence of such face-sheet/core interface debonds. Furthermore, and more importantly, there is a great need for the development of methodologies and design features that enable the mitigation of the effects of propagating interface cracks as described. This has led to an increased interest in the interfacial debond behaviour of sandwich structures, which again has led to several research studies adopting both analytical/numerical and experimental approaches.

The framework of fracture mechanics has been commonly used to describe the conditions of interfacial debond/crack propagation and arrest [2-7], where numerical modelling has been used to simulate interface crack growth in the most recent studies. Several methods have been proposed based on Finite Element (FE) analysis to simulate interface crack propagation. Examples include the Virtual Crack Closing Technique (VCCT) [8] and the Crack Surface Displacement Extrapolation method (CSDE) [9-10] The cycle jump technique, developed by Moslemian [11-14], has been proposed and utilized to reduce the number of loading cycles that need to be analysed in fatigue simulations.

In a recent study of a proposed crack arresting device, a CZM method was utilized to calculate the crack propagation and mitigation due to fibre bridging for an increasing crack length [15-17]. Other crack arrester concepts were proposed in [18-20], where FE analysis was used to demonstrate the efficiency of the crack arresting elements. In all studies [18-20] the energy release rate and the crack mode mixity angle were considered, since these physical measures are needed to quantitatively describe the conditions under which an interfacial crack will propagate. Yet another embedded sandwich crack arresting device (or peel stopper) utilizing a compliant core insert was discussed in [21], were analytical and FE methodologies were used to characterize the conditions for interface crack deflection at the tri-material junction present at the peel stopper tip. In [21] a "prediction surface" was proposed for different mode mixities and deflection angles, and based on this it was shown that crack deflection at the tri-material junction can be predicted. A common feature of the referenced research is that modelling of the entire fatigue load sequence including interface crack propagation, arrest and post arrest behaviour were not attempted.

In this study the CSDE method together with the cycle jump technique [11-14] is used to simulate interface crack propagation in foam cored sandwich beams with embedded interface crack devices (hereinafter referred to as peel stoppers) subjected to fatigue loading conditions. The emphasis is to investigate the effect of the embedded peel stopper, considering the conditions under which crack propagation, crack deflection as well as crack arrest can occur. The numerical results will be correlated with and compared against the results of a recent experimental study [22]. The aim is to demonstrate that numerical simulations can be used to assess and predict the behaviour of embedded peel stoppers and their effect on the fatigue life of sandwich structures. The peel stopper elements proposed in this work are based on the concept proposed in [21], but modified to enhance the crack deflection and arresting capabilities [23]. The models developed in this paper are used to predict the fatigue life of sandwich beams with embedded peel stoppers and are built to reflect the experimental observations made in [22] such as the crack propagation path. The numerical predictions are compared with the experimentally observed crack propagation and fatigue behaviour reported in [22]. In this paper, crack propagation and crack arrest are modelled based on a modification of Paris' law, while the post crack arrest behaviour is predicted based on fatigue data (S-N curve) for the sandwich foam core material.

EXPERIMENTAL RESULTS

Fatigue testing and crack propagation behaviour

A brief summary of the results of the experimental investigation conducted in [1] is given in this section. The novel peel stopper manufactured from pre-moulded Polyurethane (PU) resin [23], Figure 1, was implemented in foam cored sandwich beam specimens subjected to fatigue loading conditions using the Sandwich Tear Test (STT) test setup, Figure 2. The sandwich specimens consisted of identical glass fibre reinforced (GFRP) face-sheets and a PVC foam core material (Divinycell® grade H100 with a density of 100 kg/m^3 from DIAB), and a total of four specimens were tested. The crack initiation and

propagation was similar for all the tested specimens encompassing the following sequence of events, which is illustrated in Figure 3. The initial crack propagated in the face-sheet/foam interface, just below the resin rich area that is created between the face sheet and the core material, until it reached the peel stopper tip, where the crack was deflected by the peel stopper. The crack then continued propagating along the PU/foam interface until it reached the end of the peel stopper where the propagation was stopped at the crack arrest point. The fatigue loading level was subsequently increased and the fatigue test was continued until a new crack initiated on the back side of the peel stopper. The new crack then propagated into the undamaged part of the sandwich core leading to a complete failure. For each specimen, the peel stopper was evaluated with respect to the number of cycles where the crack stayed arrested at the arrest point before the re-initiation occurred (i.e. the number of cycles encountered between crack arrest and crack re-initiation), and this was compared with the overall fatigue life of the specimen. White light cameras were used to capture images during the fatigue experiments, and a digital image correlation (DIC) was established between the measured strains and the efficiency of the peel stopper.

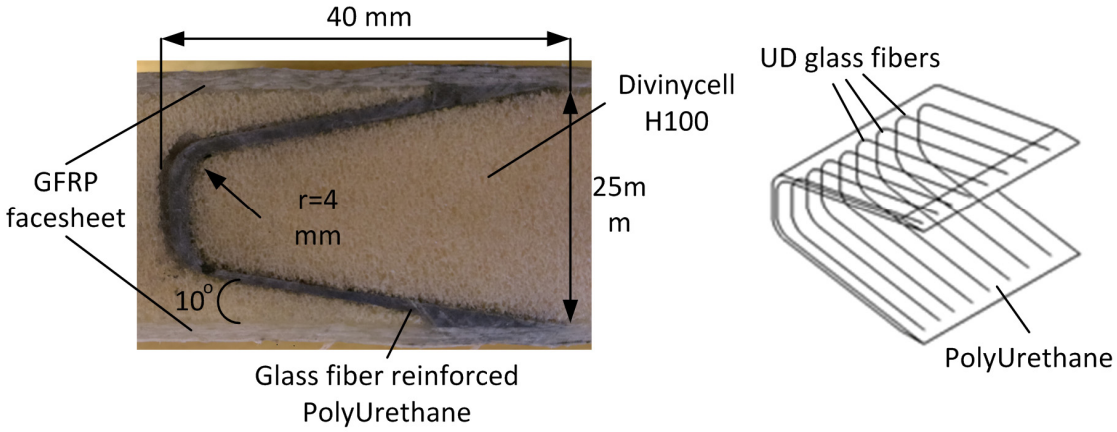

Figure 1. Peel stopper shape and material alignment.

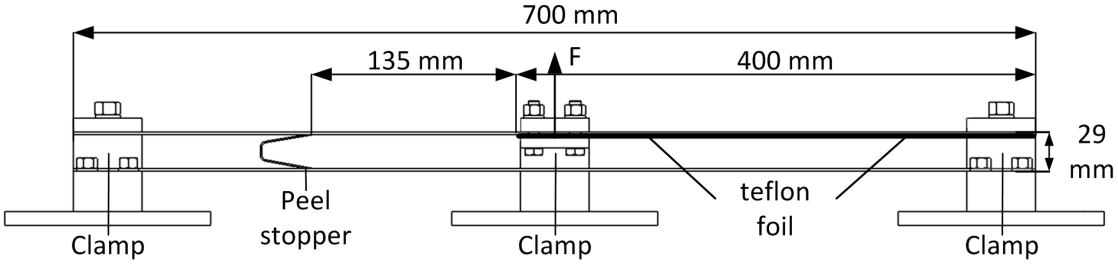

Figure 2. Sandwich Tear Test (STT) specimen dimensions and test setup.

As mentioned above, the STT specimens were loaded in load controlled fatigue at two different loading amplitudes; the first driving the crack propagation along the face-sheet/core interface until the peel stopper tip is reached, referred as load sequence A, and the second higher loading amplitude imposed to propagate the crack along the PU (peel stopper)/foam interface until the crack arrest point is reached, referred to as load

sequence B. Table 1 summarizes the two fatigue load sequences imposed, as well as the load ratio and frequency of the fatigue tests.

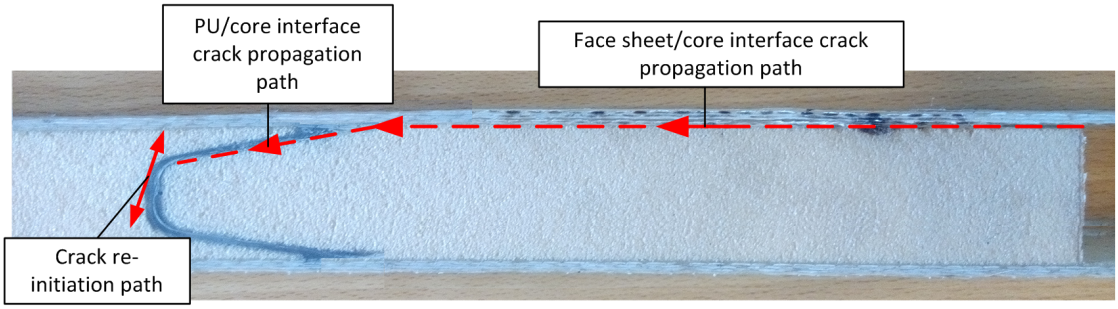

Figure 3. Crack propagation path in STT sandwich beam specimens imbedded with crack stoppers.

Table 1. Fatigue test load conditions

Fatigue test data	First fatigue load / Sequence A	Second fatigue load / Sequence B
Fatigue maximum load	380 N	950 N
Fatigue minimum load	76 N	190 N
Load Ratio	0.2	0.2
Frequency	2 Hz	2 Hz

NUMERICAL MODELLING

FE model

The finite element model has been developed in the commercial FE package ANSYS 15.0 [24]. The model is used to identify the crack loading conditions including the energy release rate (ERR) and the mode mixity phase angle as functions of the crack length. To simulate fatigue crack growth in the face-sheet/foam and PU/foam interfaces a re-meshing algorithm is used. Since the crack in all the experiments [22] propagated along the face-sheet/core interface until it reached the peel stopper tip, after which the crack was deflected along the PU/core interface, the debonded area in the FE simulations follows the path of the peel stopper angle (see Figure 4 a). The FE model represents the STT setup without including the unloaded specimen region below the debonded face-sheet in the left side of the specimen, see Figure 4 a. The peel stopper is meshed in the core structure such that it shares nodes with the foam core elements. After crack propagation along the PU/foam interface has occurred the re-meshing allows for the

nodes to be separated. In Figure 4 b-d the crack tip elements are shown at different states of crack propagation while in Figure e-g the respective states are shown in the actual specimen.

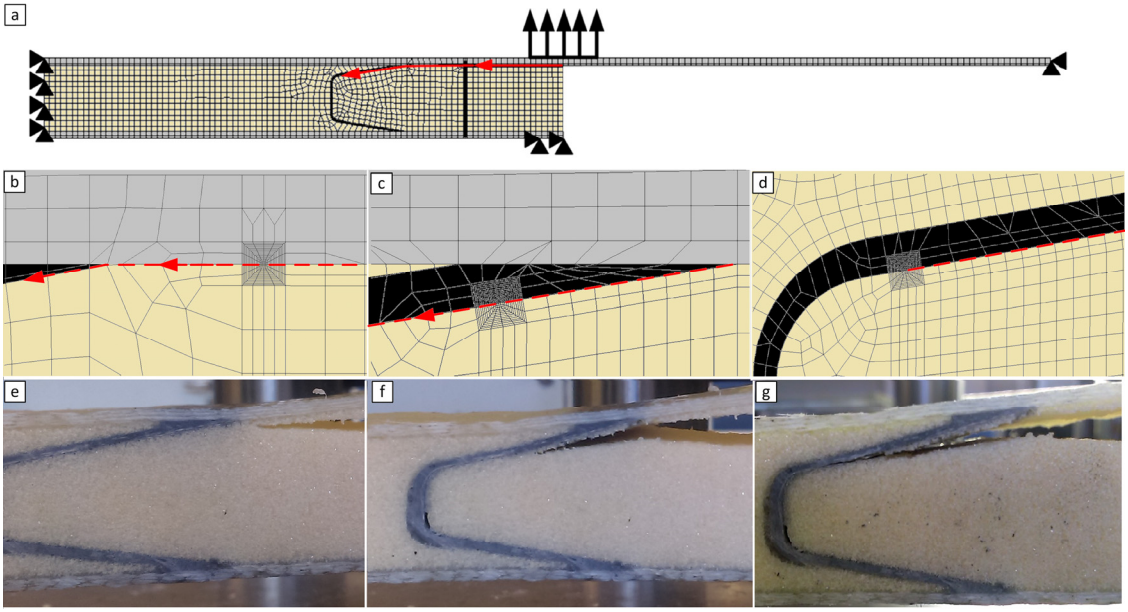

Figure 4. a) STT finite element model representation; b) and e) Crack propagating at face-sheet/foam interface; c) and f) Crack propagating at the PU/foam interface; d) and g) Crack at the arrest point.

The FE mesh is created using 8-noded plane strain elements (PLANE 183) with a global element size of 1 mm. The crack tip is meshed using element sizes down to 10 μm at the bi-material interfaces. The face-sheet and foam materials are modelled as orthotropic, while the PU/glass fibre reinforced material of the peel stopper is homogenised and modelled (approximated) as isotropic. Table 2 lists the mechanical properties of the constituent materials [22]. Geometric nonlinear behaviour is included in the FE-models to capture the in-plane membrane stresses developed in the face-sheet due large vertical displacements.

Table 2. Material properties of the constituents of the test specimens

Materials	In-plane Young's modulus (E_x)	Through thickness Young's modulus (E_y)	Shear modulus (G_{xy})	Poisson's ratio (ν_{xy})
DIVINYCELL H100	56 MPa	128 MPa	32 MPa	0.2
E-glass/epoxy	18.6 GPa	9.2 GPa*	2.7 GPa	0.4
PU	100 MPa	100 MPa	34.2 MPa	0.45

*: Assumed value

CSDE method/cycle jump technique

The Crack Surface Displacement Extrapolation (CSDE) mode mixity methodology [9-10] fits classical bi-material interface theory solutions [4,5] into a FE analysis framework to calculate directly the energy release rate (ERR) and mode mixity of a bi-material crack. In this study a special crack tip mesh is used to extract the relative nodal displacements behind the crack tip, and then use these to calculate the energy release rate (ERR) and mode mixity. The ERR and mode mixity equations as derived by the extracted relative displacements are given by [9-10]:

$$\psi_K = \arctan\left(\sqrt{\frac{H_{22}}{H_{11}}}\frac{\delta_x}{\delta_y}\right) - \varepsilon\, ln\left(\frac{x}{h}\right) + \arctan(2\varepsilon) \qquad (1)$$

$$G = \frac{\pi(1+4\varepsilon^2)}{8\,H_{11}|x|}\left(\frac{H_{11}}{H_{22}}\,\delta_y^2 + \delta_x^2\right) \qquad (2)$$

where δ_x and δ_y are the relative shear and opening displacements of the crack tip nodes behind the crack tip, $|x|$ is the distance of the crack tip node pair from the crack tip, ε is the oscillation index, and h is the chosen characteristic length [11] which is usually and for the considered analysis case is set equal to the face-sheet thickness. H_{11} and H_{22} are the parameters accounting for the anisotropic behaviour of both the face-sheet and the core material [6]. The CSDE parameter values are given in Table 3.

Finally, the cycle jump technique [11-14] is used to simulate fatigue crack growth in combination with the CSDE method. The cycle jump technique is used to reduce the number of simulated cycles in the fatigue analysis. After simulating three or more consecutive loading cycles of crack propagation, the new crack length can be calculated by linear extrapolation for a "safe" number of cycles without running the respective

simulations. This allows for saving considerable computation time when simulation of long fatigue sequences with a large number of loading cycles is needed. Previous investigations [14] have explored the sensitivity of the method to the "jump distance", and the suggestions presented are used in this study.

The propagation rate of the crack was calculated using the measured ERR, the mode mixity and a Paris' like law [25], based on energy release rate amplitude rather than stress intensity amplitude:

$$\frac{da}{dN} = m\,\Delta G^{c} \qquad (3)$$

where a is the crack length and da the crack length increment. N and dN are the loading cycles and the increment in loading cycles, respectively. Parameters m and c are fitting variables of the Paris' law curve. Finally, ΔG represents the ERR amplitude, thus the difference between the corresponding ERR levels relative to the imposed maximum and minimum fatigue load levels.

The input data for Paris' law were obtained by fatigue experiments conducted on the same bi-material interface configuration as considered in this paper using the Mixed Mode Bending test (MMB) and the G-control method developed and proposed by Manca et al. [26]. Parameters c and m are mode dependent meaning that they vary depending on the mode mixity applied. In this study the Paris law parameters were extracted for mode-I dominant crack loading conditions. It is assumed that small variations in mode mixity under general mode I loading do not affect the Paris law curve considerably. As it will be shown later, the crack propagating at the face-sheet/foam core interface (Sequence A) is highly mode I dominated. Unfortunately, fatigue data are not available for the PU/core interface over the wide range of mode mixities the crack tip is experiencing during a STT test. Alternatively, to simulate fatigue crack propagation, observations from the tested sandwich specimens are used to determine the crack growth rate along the PU/core interface, Table 3.

Table 3. CSDE and Paris' law parameters for the two interfaces.

	Face/core interface	PU/core interface
H_{11}	$1.68\cdot10^{-2}\left(\frac{1}{MPa}\right)$	$2.79\cdot10^{-2}\left(\frac{1}{MPa}\right)$
H_{22}	$1.56\cdot10^{-2}\left(\frac{1}{MPa}\right)$	$2.19\cdot10^{-2}\left(\frac{1}{MPa}\right)$
ε	$-7.066\cdot10^{-2}$	$-4.56\cdot10^{-2}$
h	2 mm	2 mm
c	$1.3758\cdot10^{-14}$	$0.9278\cdot10^{-14}$
m	4.55	4.486

FE-MODEL RESULTS AND COMPARISON WITH EXPERIMENTS

Predicted crack propagation paths

As shown in Figure 4, the crack propagation and fatigue experiment is modelled in three separate stages:

a) Crack propagation along the face-sheet/foam core interface
b) Crack propagation along the PU (peel stopper)/foam core interface
c) Crack arrest

Figure 5 shows the test machine actuator piston displacement measured for all four STT specimens [22] and the respective FE model predictions corresponding to the load application point on the debonded face sheet plotted against number of cycles for the loading sequences A (F_{max}=*380 N)* and B (F_{max}=*950 N*) respectively (corresponding to crack propagation as indicated in Figure 4a and 4b). The first part of the plot (Sequence A) represents the fatigue response of the specimens during propagation in the face/core interface and the initial stage of the fatigue life of the specimens. The second part (Sequence B) represents the fatigue response after deflection of the crack to the PU/core interface.

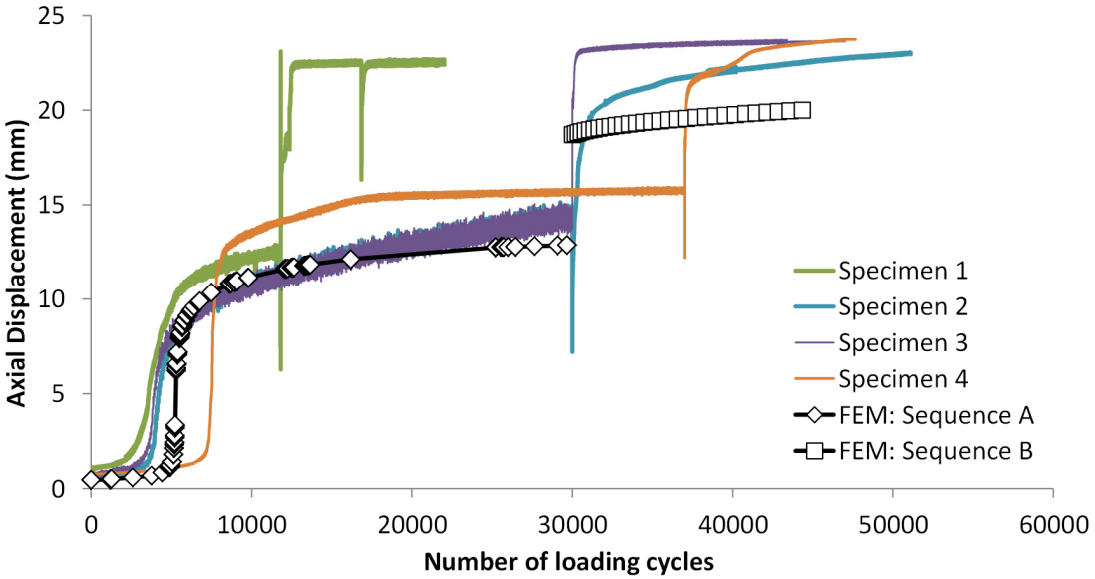

Figure 5. Vertical displacement (test machine actuator piston) vs. number of loading cycles; experimental data [1] and FE model predictions.

Figure 5 reveals an overall fair agreement between the measurements and the predictions for Specimen 2 and 3, but also that a significant variation (scatter) between the measurements for the four sandwich beam specimens exists. However, evaluating the data in Figure 5 more closely reveals that the finite element model generally under

predicts the vertical displacements slightly despite the fact that geometrically nonlinear effects are included in the modelling. This is especially pronounced for the displacements corresponding to load sequence B. The most significant cause of this discrepancy is likely to be that the vertical displacements included in Figure 5 represent the test machine piston displacement rather than displacements measured directly from the specimen. However, for the sandwich beam specimens tested in this work, the overall response does not affect the crack tip loading conditions or the stress/strain distribution in the specimen significantly as will be shown in the following. To the error of the piston measurements is investigated by a direct comparison with displacement measure from the images captured by the DIC system. Unfortunately since the images were captured at random points in time during the experiments the vast majority of the images is not taken during the maximum loading of the specimens. For this reason DIC data from the images could not be used to create the displacement vs loading cycle curves. Figure 6 shows plots that compare the displacement as recorded by the machine piston and as measured from the images of the DIC system. It can be seen that the error is very small for specimens 1 and 2 while quite significant for specimens 3 and 4. In all cases the piston measurements over predicts the actual displacement of the specimens.

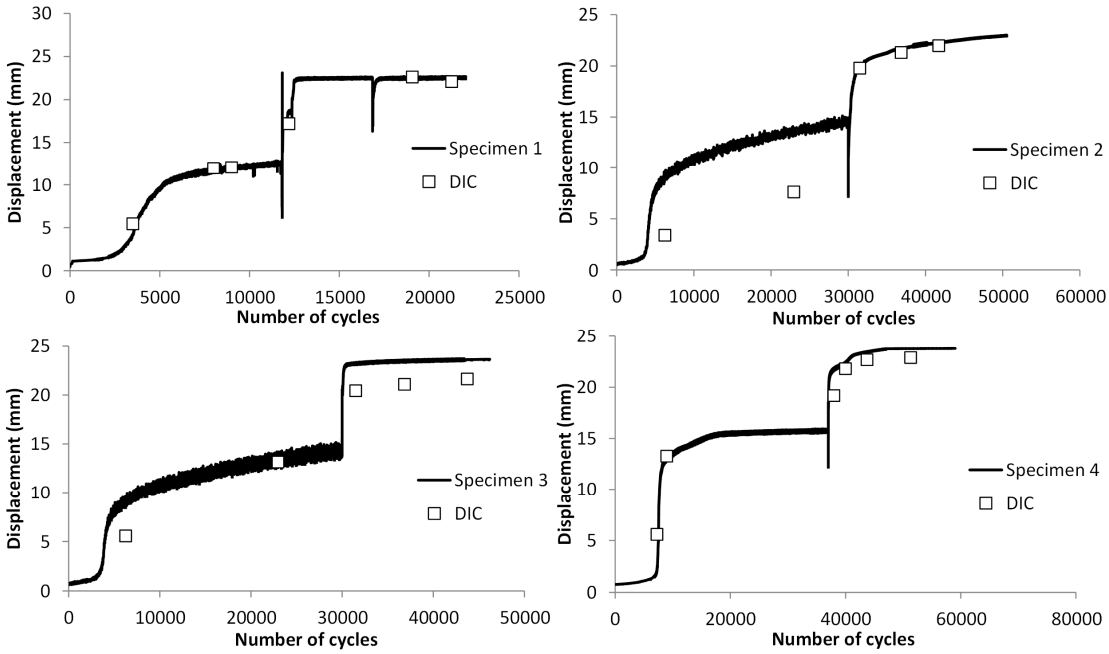

Figure 6. Comparison of displacement measured by hydraulic machines piston and images of DIC.

Energy release rate (ERR) / Mode mixity phase angle

Figure 7 and 8 show the evolution of the ERR and mode mixity phase angle as a function of the crack length (Figure 7) and number of loading cycles (Figure 8). The plots provide a good representation of the characteristic response of the STT sandwich beam specimen behaviour under load controlled fatigue testing. It is observed that the ERR rises

considerably with increasing crack length until it reaches a maximum. Past this point the vertical displacements of the debonded face-sheet have become so large compared to its thickness so that the in-plane membrane forces in the face-sheet become dominating and thus affecting the load response. Effectively the induced membrane forces stiffen the face-sheet and specimen response significantly (geometrically nonlinear effect) and consume the majority of the strain energy in the specimen, and consequently reduce the resulting ERR at the crack tip. In effect this is the reason why it was chosen to increase the imposed load at stage b (cf. Figure 4 – corresponding to load Sequence B), when the crack propagates into and along the PU/foam interface [22]. The higher load counters the increased resistance to out of plane displacements of the facesheet due to the membrane forces. If the load amplitude was kept constant as per Sequence A, the crack would arrest due to the continuously decreasing ERR. The observed abrupt change in ERR, seen from both the FE results and the experimental observations, is a result of this sudden increase of the imposed load. It is further observed that the ERR decreases again until the crack arrest point is reached.

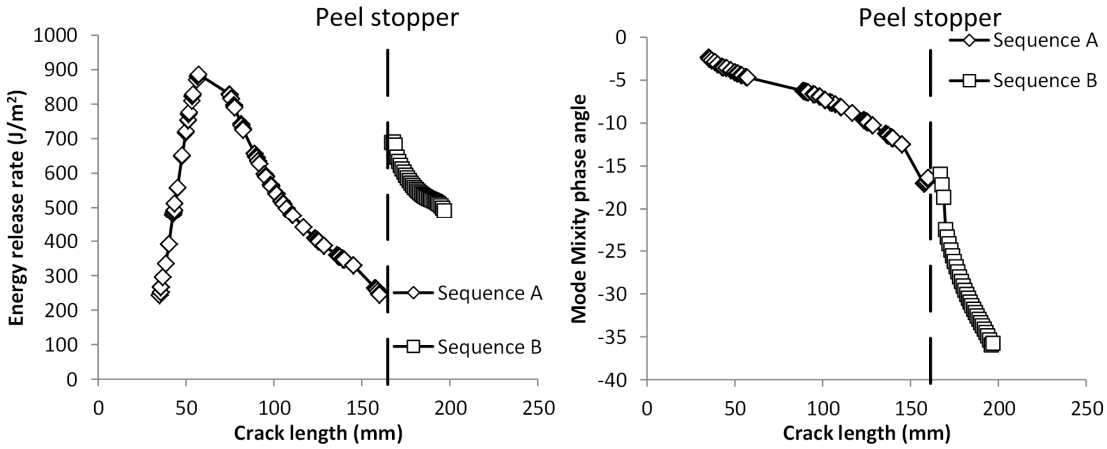

Figure 7. Energy release rate and mode mixity phase angle vs. Crack length for loading sequences A and B

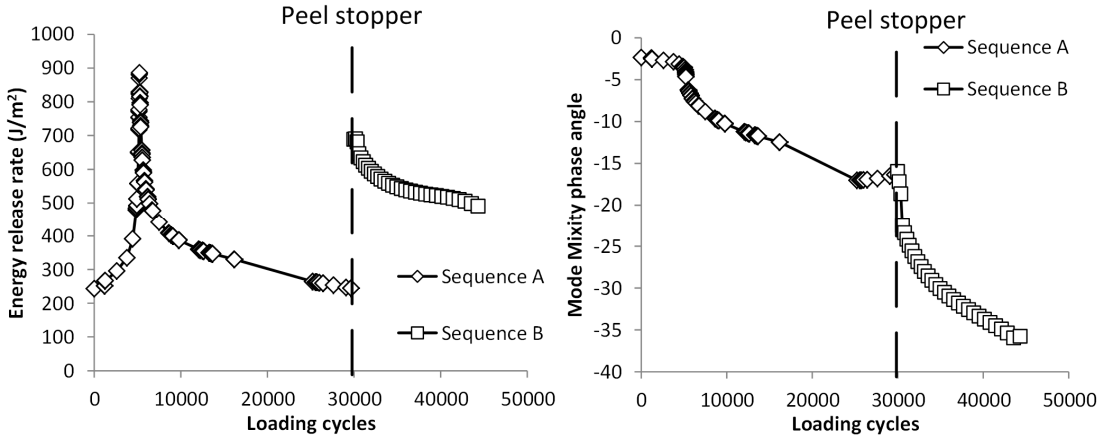

Figure 8. Energy release rate and mode mixity phase angle vs. Number of loading cycles for loading sequences A and B.

The mode mixity at the crack tip changes considerably as the crack length increases. The shear component (mode II) initially is small but increases fast. Especially at stage b (cf. Figure 4) or during Sequence B where the crack has already been deflected, the mode mixity increases negatively very rapidly, since the crack is propagating at a 10^{O} angle towards the inner part of the sandwich core material. This rapid change in mode mixity phase angle means that it is cumbersome to define the crack propagation rate to be expressed by Paris' law, since the crack propagation rate is highly dependent of both the ERR and the mode mixity. A large number of iterations of fatigue experiments are required to define the Paris Law parameters of an interface under a wide range of mode mixity phase angles Finally, the observed increase of the negative mode-II component at the crack arrest point shows a distinct and very significant tendency of the crack to return to the upper face-sheet/core interface. Under such loading conditions the high fracture toughness of the PU/GFRP peel stopper, achieved by embedding glass fibre reinforcement in the PU material [23], is essential for the performance of the peel stopper. The peel stopper itself is not displaying any sign of crack initiation, but a new crack is instead initiated in the core material on the back side of the peel stopper. That makes stage c (cf Figure 4) of the experiment last for a considerably longer period of cycles than stages a and b. That is because new cracks usually initiate a lot slower than they propagate under the same loading conditions. The main goal of embedding glass fibres in the PU material of the peel stoppers was to increase its fracture toughness and prohibit crack propagation at stage c.

FE VS. EXPERIMENTALLY CAPTURED STRAINS – CRACK RE-INITIATION AND LIFETIME PREDICTIONS

Comparison between FE model predictions and DIC measurements

The major principal strains in the core material behind the peel stopper are derived from the FE analysis of the sandwich specimen with the crack located at the arrest point, i.e. stage c (cf. Figure 4). Figure 9, shows the field of major principal strains obtained from the DIC measurements for specimens 1-4 during the conducted fatigue tests [22], and the corresponding field of major principal strains predicted using the FE model. It is observed that the characteristic strain concentration observed in the core material on the back side of the peel stopper in the experiments, is also observed from the FE simulation results. Moreover, the FE model predicts principal strain values that are close to the average of the values measured using DIC. It should be noted that the discrepancy between the strain fields observed for the physical specimens can be attributed to the slightly different propagation paths observed and experimental scatter [22]. The foam material exhibits local variations of mass density and therefore local stiffness variations, and this also contributes to explain the differences between the observed strains. In all cases the observed strain concentrations are caused by local bending of the peel stopper and are not the result of the stress concentrations at the crack tip. To predict the crack

arrest time, i.e. the number of cycles between crack arrest and crack re-initiation behind the peel stopper (i.e. number of cycles where the crack remains at stage (c), cf. Figure 4), it is necessary to relate the peak strain values to the occurrence of crack re-initiation. Since the development of a crack re-initiation modelling algorithm was not part of this work, the estimation of the remaining fatigue life is conducted through the use of fatigue data obtained for the Divinycell® H100 PVC foam material [27,28].

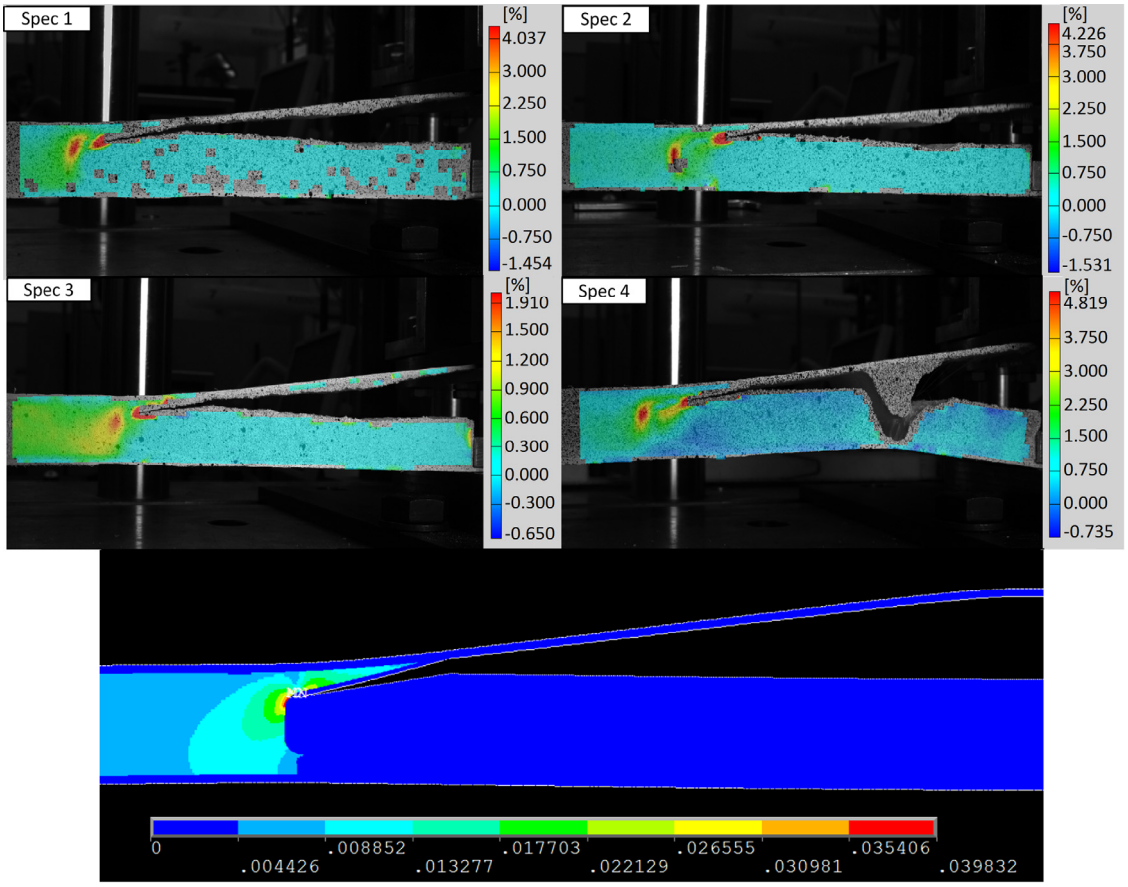

Figure 9. Comparison of FE predictions and measured major principal strain fields (DIC – [1]) at crack re-initiation behind the peel stopper.

Maximum strain

The FE model was used to predict the major principal strain field, as depicted in Figure 10, for several different crack lengths extending between the peel stopper tip and the crack arrest point. The maximum values of the major principal strain were recorded for both the maximum and minimum fatigue load values as defined by Table 1. This is not to be confused with the two different fatigue load amplitudes (load Sequences A and B) used during the testing in [22]. The maximum and minimum loads discussed here represent the fatigue load limits corresponding to the second fatigue load amplitude level (sequence B), i.e. F_{max}=950N, F_{min}=190N. In Figure 10a the maximum and minimum major principal strains, ε_{max} and ε_{min}, at the crack re-initiation point in the core are plotted

against the number of loading cycles. In Figure 10b, the corresponding strain ratio $R_\varepsilon=\varepsilon_{min}/\varepsilon_{max}$ plotted against the number of loading cycles is shown.

It is observed that the strains at the crack re-initiation point increase when the crack approaches the crack arrest point. Since at stage (c) the crack is not propagating (it is arrested), the strain values remain constant for the remaining part of the arrest time, until a new crack initiates behind the peel stopper. As discussed previously, the crack re-initiating behind the peel stopper can be associated with the major principal strain values. Accordingly, the strain ratio (defined as $R_\varepsilon=\varepsilon_{min}/\varepsilon_{max}$) at the re-initiation point is of high interest. It is seen that R_ε does not remain constant as the crack propagates along the peel stopper, and it reaches its maximum value at the crack arrest point where it is equal to R_ε=0.39. It should be noted that the applied load ratio in the experiments and also in the FE-model is constant at R_L=0.2.

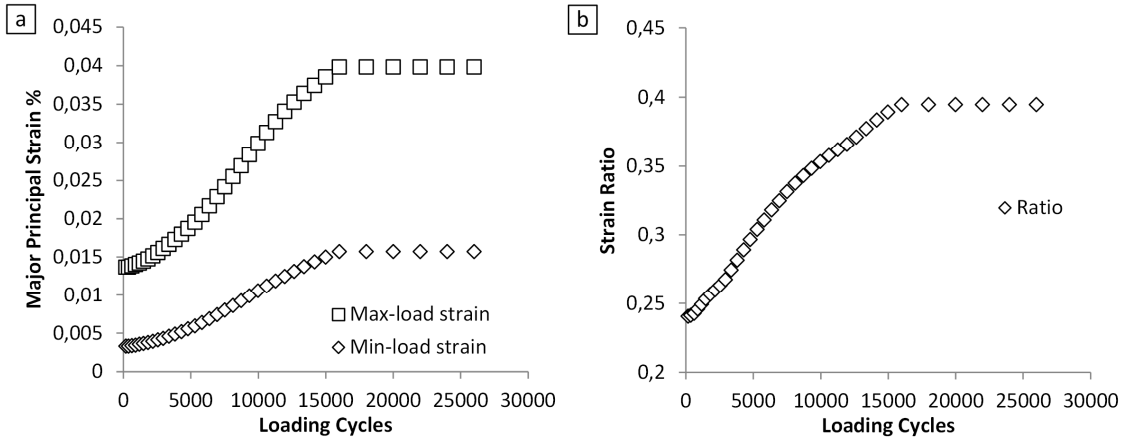

Figure 10. Major principal strains and the strain ratio at the crack re-initiation point corresponding to the maximum and minimum fatigue load levels during fatigue testing vs. number of load cycles.

Arrest time prediction

To estimate the total time of crack arrest (or the number of cycles between crack arrest and crack re-initiation) based on the calculated strains, shear strain fatigue data are considered according to [27] and [28]. The data correspond to shear strain fatigue tests of H100 Divinycell PVC foam material conducted on sandwich beams in four-point bending. The stress or equivalently the strain ratio during the fatigue tests was defined at R_s=0.1. To account for the effect of the strain ratio on the fatigue damage accumulation in the foam and to effectively compare the strains calculated from the FE analyses to the H100 fatigue data, the maximum to minimum strain difference (or strain range) is calculated:

$$\Delta\varepsilon = (1 - R) * \varepsilon_{max} \qquad (4)$$

where ε represents the shear strain from the fatigue data as well as the major principal strains from the DIC measurements and the FE analyses. Figure 11 shows observed strain

range vs. the number of cycles when the crack was arrested (between crack arrest and re-initiation) in comparison with the H100 shear fatigue data. The shear fatigue data curve in combination with the calculated FE model strain are used to predict the number of cycles before crack re-initiation and at the crack arrest point, and this is also shown in Figure 11 (orange circle).

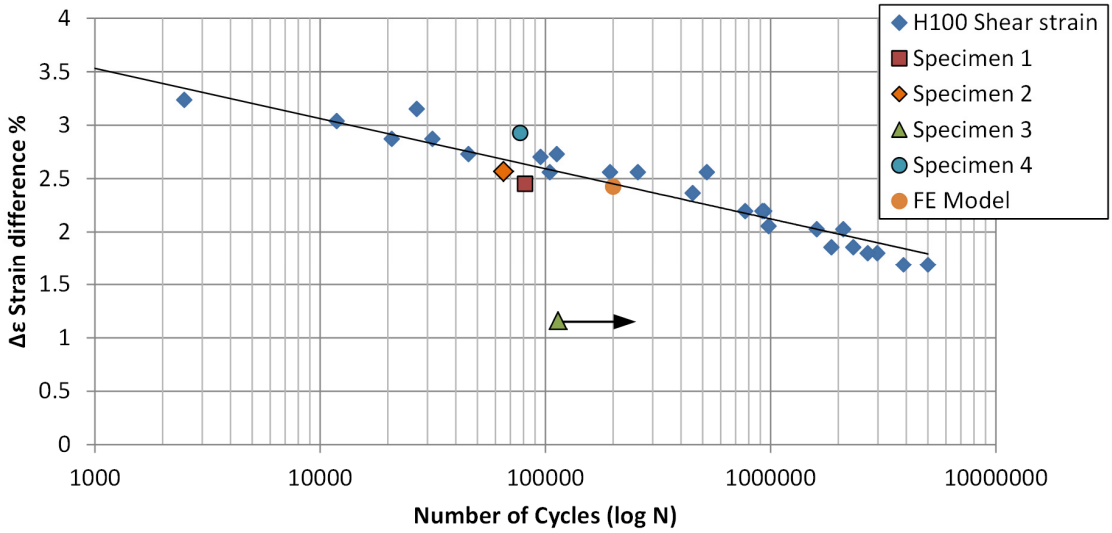

Figure 11. Strain range vs.-number of cycles while crack is arrested; measurements [1], FE model results and comparison with H100 shear fatigue data.

From Figure 11 it is observed that according to the FE model predictions for the average sandwich specimen can be expected to withstand a total of approximately 200,000 load cycles in arrested state before crack re-initiation occurs. This corresponds to almost 3 times the number of cycles to crack arrest, and this effectively implies that the embedded peel stopper has almost doubled the expected fatigue life of the specimens in comparison with sandwich specimens without embedded peel stoppers. The four sandwich beam specimens tested and reported in [1] experienced between approximately 65,000 and 114,000 load cycles at the arrested state, and this implies that FE-model in combination with the H100 fatigue data overestimates the number of load cycles to crack re-initiation. The likely reason for this is that the fatigue shear data for the H100 PVC that was used together with the FE model was obtained from a four-point shear test, and this test configuration does not provide an accurately representation of the stress/strain state at the crack re-initiation point behind the peel stopper. This demonstrates that the performance and efficiency of the peel stopper concept proposed is very sensitive to the actual strain state developing at the crack re-initiation point. Accordingly, a small change (reduction) of the peak strains developing behind the peel stopper, which can be achieved by careful design optimisation of the peel stopper geometry/configuration, has the potential of increasing the expected fatigue life considerably.

CONCLUSIONS

The basis and motivation for the research presented is a recent experimental study [22] concerning the performance of a novel peel stopper (crack arresting device) for foam

cored composite sandwich structures. The principal findings of this investigation has formed the basis for the research presented in this paper, which encompasses the proposition of both a numerical modelling strategy, as well as a classification of the different stages of the crack initiation and propagation process for the foam cored sandwich beams with embedded peel stoppers. In particular, the numerical simulation methodology developed in this research enables the prediction of the fatigue response and expected fatigue life of foam cored composite sandwich beams with embedded peel stoppers subjected to fatigue loading. The numerical modelling includes fatigue crack propagation simulation along two bi-material interfaces, crack kinking simulation as well as strain field extraction for the prediction of crack initiation. The experimental data obtained from the sandwich beam specimen tests conducted using the STT setup in [22] have been used to validate the FE models predictions. Overall the numerical predictive results compare well with the experimental observations. Moreover, it is demonstrated that the post crack arrest behaviour can be predicted. The results further suggests that there is a significant potential for improving the peel stopper design leading to increased efficiency (and thereby increased fatigue life expectancy) by optimisation of peel stopper geometry/configuration, since the results demonstrate that crack re-initiation behind the peel stopper depends very much on the local strain state.

The findings of this research are important for future development and application of peel stoppers (crack arrest devices) in more representative real application sandwich structures (like e.g. sandwich panels that may be flat or curved). The proposed modelling methodology can be very useful in achieving this, as it can be used for design evaluation as well as optimisation of the shape and position of peel stoppers embedded into complex sandwich components, sub-structures or larger assemblies.

ACKNOWLEDGEMENTS
The work was sponsored by the Danish Council for Independent Research | Technology & Production Sciences (FTP) under the research grant “Enhanced performance of sandwich structures by improved damage tolerance" (SANTOL) (Grant 10082020). The Divinycell H100 material used in this study was provided by DIAB Group, Sweden. The work has been conducted in collaboration with and co-sponsored by the Technical University of Denmark, Aalborg University, Denmark, the University of Southampton, UK, Siemens Wind Power A/S, Denmark, and LM Wind Power Blades A/S, Denmark.

REFERENCES

[1] Zenkert, D., “An introduction to sandwich construction” London: Chameleon Press Ltd, 1995
[2] Erdogan, F., 1971. Bonded dissimilar materials containing cracks parallel to the interface, *Engineering Fracture Mechanics*, 3, 231-240.
[3] Dundurs, J., 1969. Edge-bonded dissimilar orthogonal elastic wedges. J.Appl.Mech. 36, 650-652.

[4] Hutchinson J.W., Suo Z., 1992. Mixed Mode Cracking in Layered Materials", Advances in Applied Mechanics, 29, 63-191.
[5] He M.Y., Hutchinson J.W., 1989. Kinking of a crack out of an interface, J. appl. Mech., 56, 270–278.
[6] Suo, Z., 1990. Singularities, interfaces and cracks in dissimilar anisotropic media. Proceedings of the Royal Society of London A: Mathematical, Physical and Engineering Sciences 427 (1873), 331-358.
[7] Wang, T. C., 1994. Kinking of an interface crack between two dissimilar anisotropic elastic solids. International Journal of Solids and Structures 31 (5), 629–641.
[8] M. Rinker, R. Krueger, J. Ratcliffe, 2013. Analysis of an Aircraft Honeycomb Sandwich Panel with Circular Facesheet/Core Disbond Subjected to Ground-Air Pressurization, NASA/CR-2013-217974, NIA report no. 2013-0116.
[9] Berggreen C., 2004. Damage tolerance in debonded sandwich structures. PhD. Thesis. Department of Mechanical Engineering, Technical University of Denmark.
[10] Berggreen, C., Simonsen, B. C., Borum, K. K., 2007. Experimental and numerical study of interface crack propagation in foam-cored sandwich beams. Journal of Composite Materials 41 (4), 493–520.
[11] Moslemian, R., Karlsson, A. M., Berggreen, C., 2011. Accelerated fatigue crack growth simulation in a bimaterial interface. International Journal of Fatigue 33 (12), 1526–1532.
[12] Moslemian, R., Berggreen, C., 2013. Interface fatigue crack propagation in sandwich X-joints – Part I: Experiments. Journal of Sandwich Structures and Materials, 15(4), 429-450.
[13] Moslemian, R., Berggreen, C., 2013. Interface fatigue crack propagation in sandwich x-joints – Part II: Finite element modeling. Journal of Sandwich Structures and Materials 15 (4), 451-463
[14] Moslemian, R., 2011. Damage Tolerance of Curved Sandwich Structures in Wind Turbine Blades. PhD. Thesis. Department of Mechanical Engineering, Technical University of Denmark.
[15] Lundsgaard-Larsen, C., Berggreen, C., Carlsson, L. A. 2010. Tailoring Sandwich Face/Core Interfaces for Improved Damage Tolerance: Part I: Finite Element Analysis. Applied Composite Materials, 17(6), 609-619.
[16] Lundsgaard-Larsen, C, Berggreen, C & Carlsson, LA 2010, 'Tailoring Sandwich Face/Core Interfaces for Improved Damage Tolerance: Part II: Experiments' Applied Composite Materials, vol 17, no. 6, pp. 621-637.
[17] Lundsgaard-Larsen, C., Berggreen, C., Carlsson, L. A. 2010. Tailoring Sandwich Face/Core Interfaces for Improved Damage Tolerance: Part II: Experiments. Applied Composite Materials, 17(6), 621-637.
[18] Rinker, M., Zahlen, P. C., John, M., Schäuble, R., 2012. Investigation of sandwich crack stop elements under fatigue loading. Journal of Sandwich Structures and Materials 14 (1), 55–73.
[19] Hirose Y, Matsubara G, Hojo M, Matsuda H, Inamura F., 2008. Evaluation of modified crack arrester by fracture toughness tests under mode I type and mode II type loading for foam core sandwich panel. In: Proc. US-Japan conference on composite materials 2008, Tokyo, Japan.

[20] Hirose, Y., Matsuda, H., Matsubara, G., Hojo, M., Inamura, F., 2012. Proposal of the concept of splice-type arrester for foam core sandwich panels. Composites Part A: Applied Science and Manufacturing 43 (8), 1318–1325.
[21] Jakobsen, J., Andreasen, J. H., Thomsen, O. T., Sep. 2009. Crack deflection by core junctions in sandwich structures. Engineering Fracture Mechanics 76 (14), 2135-2147.
[22] Martakos G., Andreasen, J. H., Berggreen C., Thomsen, O. T., Experimental Investigation of Interfacial Crack Arrest in Sandwich Beams Subjected to Fatigue Loading using a Novel Crack Arresting Device.
[23] Wang, W., Martakos, G., Dulieu-Barton, J.M., Andreasen, J.H. and Thomsen, O.T., 2015. Fracture behaviour at tri-material junctions of crack stoppers in sandwich structures. Composite Structures, 133, 818-833. 10.1016/j.compstruct
[24] ANSYS® Academic Research, Release 15.0
[25] Paris P., Erdogan F., 1963, A critical analysis of crack propagation laws, J Basic Engng Trans ASME Ser D, 85 (4) 528–534.
[26] Manca, M., Berggreen, C., Carlsson, L. A., 2015. G-control fatigue testing for cyclic crack propagation in composite structures. Accepted for publication in Engineering Fracture Mechanics. DOI 10.1016/j.engfracmech
[27] Burman, M., Magnusson, B., 2008. Fatigue testing of H60, H100 and H200. Technical report (DIAB), KTH (Sweeden).
[28] DIAB. Divinycell H-Grade Technical data, 2014. Laholm (Sweeden) (http://www.diabgroup.com).